1   **Assessing the reliability and uncertainties of projected changes in precipitation and**
2   **temperature in CMIP5 models over the Lake Chad basin**

3

4   Elias Nkiaka[1], Rizwan Nawaz[2] and Jon C. Lovett[1]

5   [1]School of Geography, University of Leeds.

6   [2]Department of Civil & Structural Engineering, University of Sheffield

7   Correspondence to: Elias Nkiaka (gyenan@leeds.ac.uk)

8

9   **Abstract**
10   Lake Chad lost more than 80% of its surface area over the past decades as a result of environmental
11   change and climate variability. It is not yet known how climate change will affect water resources
12   availability in the basin over the coming decades. In this study, the Reliability Ensemble Averaging
13   (REA) technique was used to evaluate the performance of CMIP5 models in simulating present-day
14   precipitation and temperature (1980 – 2005); and to quantify the uncertainties in future projections
15   (2050 – 2075) under two Representative Concentration Pathways (RCPs) in the Lake Chad basin
16   (LCB). Analyses were carried out at both annual and seasonal time-scales. Overall, the CMIP5
17   models simulated precipitation better than temperature in the study area. Although the models were
18   able to simulate the annual precipitation cycle in the basin, most models overestimated precipitation
19   during the dry season and underestimated it during the monsoon season. Future annual basin
20   precipitation is projected to increase by 2.5% and 5% respectively under RCP4.5 and RCP8.5
21   scenario by the middle of the century by most of the models and most of the model projections are
22   within the REA uncertainty range. Despite the increase in projected annual precipitation in the basin,
23   most models project a decrease in monsoon precipitation under both RCPs. Although the uncertainty
24   range for future precipitation projections for most models lie within the range of natural climate
25   variability, additional analysis are needed for results to be useful for any future planning in the study
26   area.

27

28   **Keywords:** Lake Chad basin, reliability ensemble averaging, uncertainty quantification, CMIP5,
29   climate projections, climate change, simple model averaging

1. Introduction

31   Climate change is expected to cause major disruptions to the global hydrological cycle as a
32   result of changes in precipitation patterns with the impacts expected to be exacerbated by rising

global population (Arnell 2004; Trenberth 2011; Gosling and Arnell 2016). For example in some tropical regions like the Sahel, the frequency of storm events has increased by three folds over the past three decades as a result of global warming (Taylor et al. 2017). Therefore, developing future water resources management and planning strategies under anticipated climate change requires the estimation of current and future precipitation magnitude and variability (Wehner 2013). This can be achieved through the application of Global Circulation Models (GCMs) which are used to predict climate change associated with future scenarios of greenhouse gas concentrations (Siam et al. 2013). For these climate models to be used for impact studies, they need to be evaluated against observed data to assess their performance in simulating the present-day climate. Even so, it has been reported that GCM skill in simulating the present-day climate relates very weakly to its ability to simulate projected climate (Knutti et al. 2010).

Notwithstanding, different techniques have been applied to evaluate the performance of GCMs in simulating present and future precipitation and temperature changes. These methods range from simple statistical techniques e.g. mean errors, correlations, root-mean-square errors (Akurut et al. 2014) to advanced statistical techniques e.g. volumetric hit index (VHI) (Mehran et al. 2014). Such methods are used to compare model output with observations. The second widely used evaluation method is the diagnostics approach that provide information on the sources of model errors and how to identify processes connected with these errors e.g. analysis of energy and water cycles, and analysis of atmospheric and land processes (Siam et al. 2013). Another approach is the evaluation of GCMs based on their ability to simulate specific atmospheric processes such as the monsoon precipitation in the tropics, ENSO events and other atmospheric processes that influence the climate of a region (Rowell 2013).

Despite the various evaluation techniques available, a fundamental problem associated with the application of GCMs is how well they can simulate climate at the regional scale. While GCMs projections may be consistent in terms of global mean changes, they generally disagree on the magnitude, and in many cases the sign, of change at a regional scale, especially precipitation patterns (Meehl et al. 2007). This raises the issue of uncertainty associated with the use of GCMs. Many methods used for evaluating GCMs do not consider the issue of uncertainty inherent in climate models. In fact, there are many sources of uncertainties associated with the use of GCMs including: natural climate variability, variability between and within models and uncertainty caused by the future emissions of greenhouse gases (GHGs). How this uncertainty can be quantified to enhance decision making remains a challenge. It has been recognized that, uncertainty quantification is a

critical component in the description and attribution of climate change (Katz et al. 2013). The most popular method used for assessing uncertainties in GCMs projections is the application of large independent multi model ensembles (MMEs) from different modelling groups under different scenarios to determine future climate projections (Tebaldi and Knutti 2007; Knutti et al. 2010).

Generally, the approaches available for uncertainty estimation in GCMs are limited in the literature. Despite this limitation, Koutsoyiannis et al. (2007) used a combination of analytical and Monte Carlo methods to determine the uncertainty limits for temperature, precipitation and runoff projections from GCMs for a catchment in Greece. Woldemeskel et al. (2012) developed and tested the square root of error variance (SREV) method for quantifying uncertainty in future precipitation and temperature projections from GCMs at global scale. Min and Hense (2006) applied the Bayesian model averaging (BMA) technique for uncertainty assessment in global mean surface temperature from an ensemble of GCMs projection. Giorgi and Mearns (2002) developed and tested the Reliability Ensemble Averaging (REA) technique for uncertainty estimation in GCMs at regional scale.
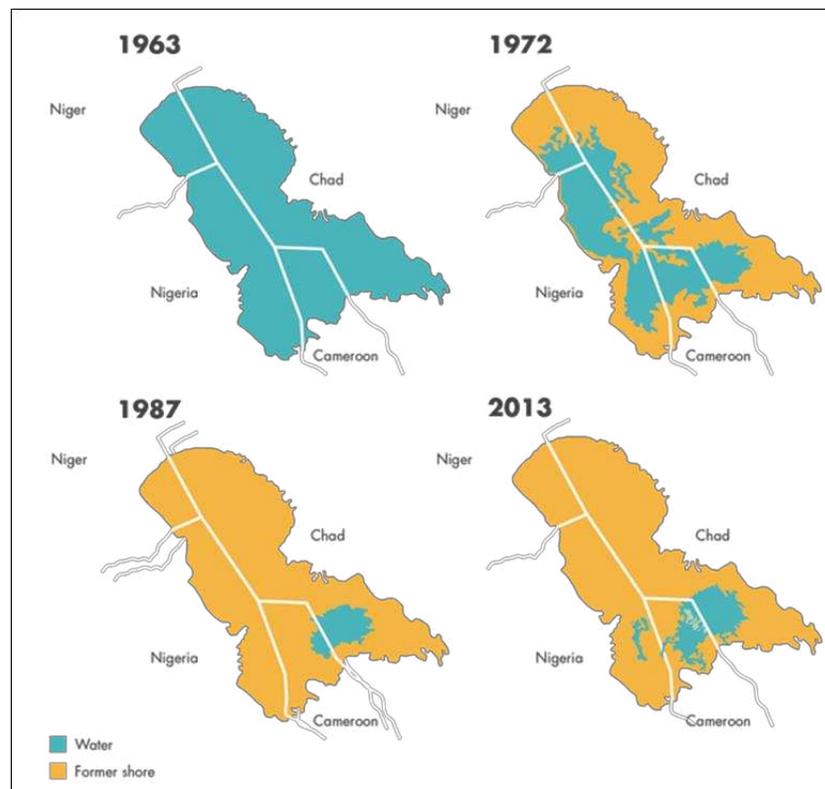
Figure 1: Desiccation of Lake Chad 1963 – 2013 (source: UNEP DIVA-GIS)

Many models participating in the fifth phase of the Coupled Model Intercomparison Project (CMIP5) (Taylor et al. 2012) have been evaluated across different regions in Africa. For example Akurut et al. (2014) evaluated precipitation estimates from CMIP5 models over the Lake Victoria, Siam et al. (2013) evaluated the performance of CMIP5 models in the Congo and Upper Blue Nile river basins, Biasutti (2013) tested the performance of CMIP5 models on the prediction of Sahel rainfall. Despite these numerous studies in Africa, none of them considered the quantification of GCM uncertainty. Meanwhile, the Lake Chad basin (LCB) remains poorly represented in those studies despite the significant changes that have been observed in the hydrological dynamics of the basin.

From 1960 to 2000, Lake Chad, an endorheic lake located in Central Africa experienced one of the most significant and sustained reduction in rainfall recorded anywhere in the world causing the lake area to shrink by more than 80% (Odada et al. 2009) (Figure 1). Despite this remarkable shrinkage, the LCB remains one of the most under-studied basins in Africa in terms of understanding the climate dynamics in the basin and how it will be affected by future climate change. This issue is further exacerbated by inadequate observational records in the region (Nkiaka et al. 2017a). Despite the scarcity in research output, Armitage et al. (2015) used paleo-climate records from the LCB to show that Lake Mega-Chad exerts a strong control on global biogeochemical cycles. Nkiaka et al. (2017b) analyzed past annual and seasonal rainfall in the southern part of the LCB and reported of a general decline in monsoon precipitation over the period 1951 – 2000. However, no study has focused specifically on future precipitation and temperature projections in the LCB using the recent or previous generations of climate models.

Even so, results from previous climate models projections for future precipitation in Central Africa have produced contrasting results. Haensler et al. (2013) evaluated an ensemble of CMIP3/5 and RCMs in the Central Africa region and concluded that no significant changes in precipitation may be observed in the region by the end of the present century under two representative concentration pathways (RCPs) RCPs 4.5 and 8.5. In a separate study; Aloysius et al. (2016), reported that CMIP5 models were projecting an increase in future precipitation by the end of the present century in the area of their study domain covering the LCB under RCPs 4.5 and 8.5. Meanwhile, using the regional climate model REMO forced by two GCMs (Europe wide Consortium Earth System Model (EC-Earth) and Max-Planck Institute Earth System (MPI-ESM)), Fotso-Nguemo et al. (2017), reported that future precipitation over the area of their study domain covering the LCB will decrease by the end of the present century under RCPs 4.5 and 8.5. Results

114   from those studies are quite contrasting and cannot be used for any impact studies to enhance
115   adaptation planning in the region, hence the necessity to carry out the present study in the LCB.

116   Although floods have become recurrent in recent years across the LCB causing widespread
117   socio-economic damages, water availability for agriculture, pastoral activities, ecosystem
118   sustainability and contribution as inflow into Lake Chad, is still under threat due to the erratic nature
119   of rainfall. In addition, water resources in the LCB are becoming increasingly vulnerable due to
120   rising population causing tension among water users (Ngatcha 2009). A study by Okpara et al.
121   (2015) has shown that climate-induced water scarcity in the LCB could combine with other human
122   factors such as population increase, poverty and political instability to create a fertile environment
123   for armed conflict. Given the increasing number of refugees in the LCB as a result of "boku haram"
124   terrorist activities in the region (OCHA 2017), climate change could aggravate the current situation
125   resulting in mass migration which could threaten global security. With these myriad of challenges,
126   there is need for research that can enhance our understanding on how precipitation and temperature
127   which determine the availability of water resources will be affected by future climate change in the
128   LCB. This is a crucial knowledge gap in the LCB that this research seeks to fill.

129   The objectives of this study were to: (i) evaluate the ability of CMIP5 models to reproduce
130   the present-day climate conditions in the LCB (1980-2005); (ii) assess the future climate projections
131   for the basin by the middle of century (2050 – 2075) relative to the historical period, and quantify
132   the uncertainties associated with these projections using two representative concentration pathways
133   (RCP4.5 and 8.5); and (iii) evaluate the performance of each ensemble member. This was achieved
134   using the Reliability Ensemble Averaging (REA) technique. The method has been used in previous
135   studies to establish uncertainty limits in GCMs projections (Giorgi and Mearns 2002; Rawlins et al.
136   2012; Miao et al. 2014). At smaller spatial scale, the technique has been used to evaluate CMIP5
137   models by (Rawlins et al. 2012; Sengupta and Rajeevan 2013; Tanveer et al. 2016). The advantages
138   of the REA technique compared to other methods include the fact that the uncertainty range around
139   the simulated changes can be reduced by minimizing the influence of ''outlier'' or poorly performing
140   models and it also offers the possibility to calculate the uncertainty range around the REA average
141
142
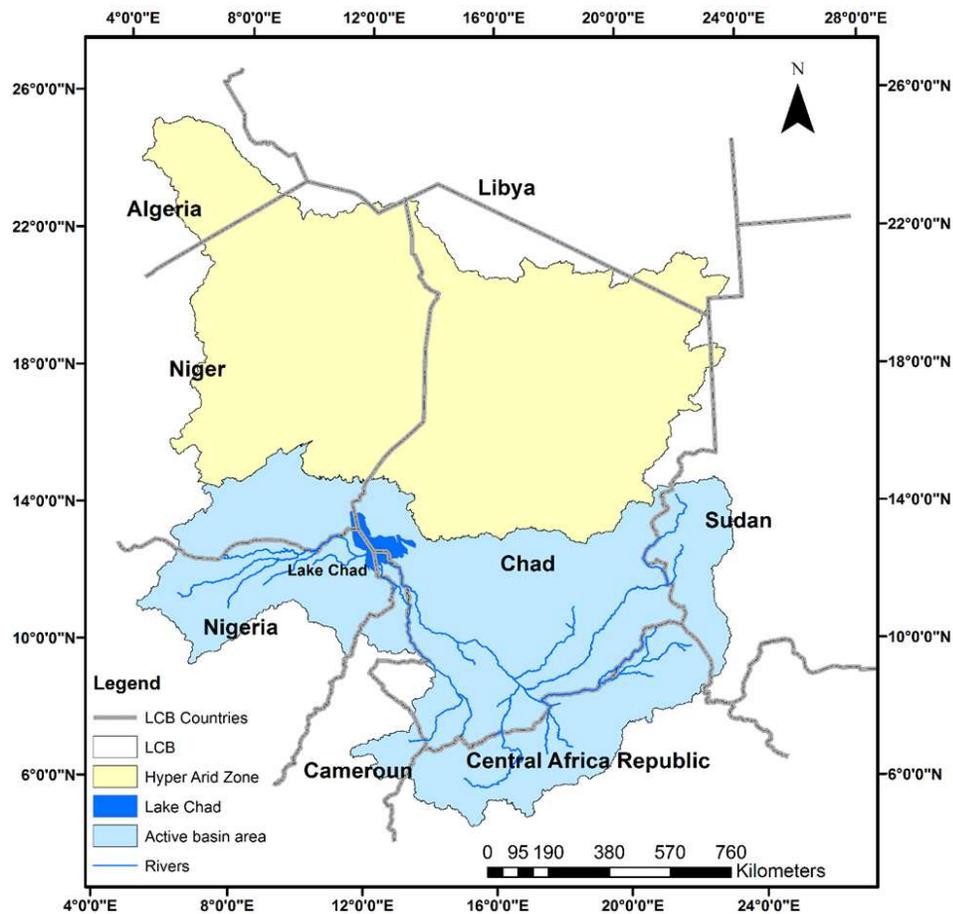
Figure 2: Lake Chad Basin: Latitudes 5-10 N (sudano), 10-12 N (semi-arid) and 12-16 N (arid)

2. Study area

The Lake Chad basin (LCB) is located in Central Africa and lies between 5° - 24°N and 7° - 24°E (Figure 2). The entire basin covers an estimated area of 2,434,000 km^2 shared by Algeria, Cameroon, Central Africa Republic, Chad, Libya, Niger, Nigeria and Sudan. This study focuses on the active drainage basin with an area of 1,053,455 km^2 (Adenle 2001) located between 5° - 16°N and 7° - 24°E (Cameroon, Central Africa Republic, Chad, Niger, Nigeria and Sudan). The reason for choosing only the active basin area is because, only this area contributes to inflows into the lake while the rest of the northern portion is covered by desert. Apart from some local mountains and plateaus located in northern and southern parts of the basin, the central part of the basin is very flat with an average slope of <1.3% (Le Coz et al. 2009; Nkiaka et al. 2017c).

Using data from Climate Research Unit (CRU) Time Series version 3.20 covering the period 1901 – 2000, average rainfall over the basin was estimated to measure about 900 mm/year, varying between 1400 mm/year in the south to 370 mm/year in the north while average temperature was

estimated at 26.5°C. Figure 3 shows the contour plots of annual precipitation and average surface temperature for the active basin area averaged over the period 1980 – 2005. The raining season in the basin usually lasts from May to October with the highest rains recorded in August. The climate in the basin is mostly hot and dry and rainfall is controlled by the north-south seasonal migration of the intertropical convergence zone (ITCZ) as observed in the Logone catchment (Nkiaka et al. 2017b). 95% of inflows into the lake is contributed by the Logone and Chari rivers which originate from the south (Odada et al. 2009).

Due to the high spatial variability in precipitation across the LCB, for the purpose of this study, the active drainage basin was divided into three different ecological zones: 5° - 10°N "Sudano", 10° - 12°N "semi-arid" and 12° - 16°N "Arid". These ecological zones represent some simplified climatic zones based on Köeppen Geiger's climate classification for Africa (Peel et al. 2007). Rainfall across all the ecological zones is unimodal with the peak occurring in August. The highest rainfall is recorded in the Sudano zone while the lowest occurs in the arid zone. The CMIP5 models were assessed at the basin level and for each ecological zone. The advantage of this approach is that in regions with high spatial variability and strong rainfall gradients such as the LCB, model output averaged over the whole basin may lead to loss of signal such that the true expected change could be larger than what is suggested by the model average (Knutti et al. 2010).
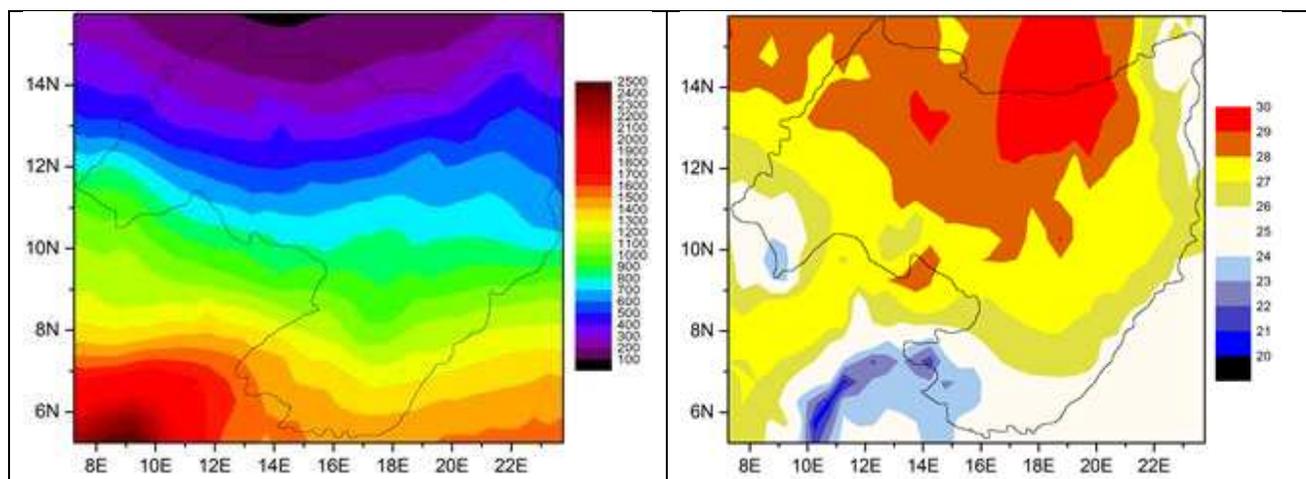
Figure 3: Contour plots for annual precipitation (left panel) and average surface temperature (right panel) in the active basin area (1980 – 2005) calculated from CRU

3. Data

3.1. Observed Data

Due to the scarcity of observational data in the LCB, the observed rainfall and temperature data used in this study was derived from climate research unit (CRU) Time Series version 3.20 dataset described by Harris et al. (2014) and made available free of charge by the British Atmospheric Data Centre. This provides monthly-mean precipitation totals and average temperature on a resolution of (0.5x0.5 degree) grids for the period 1901–2011. This dataset has been used as the reference to evaluate CMIP5 models in previous studies e.g. (Rowell 2013; Miao et al. 2014; Pattnayak et al. 2017). An additional precipitation dataset Watch Forcing Data methodology applied to ERA-Interim (WFDEI) (Weedon et al. 2014) was used to complement the CRU dataset. WFDEI has been applied for hydrological modelling studies in the Lake Chad basin (Nkiaka et al. 2017a) and can be obtained from https://dataguru.lu.se/.

Table 1: List of climate models used in the study

Model No	Model Name	Institute/Country	Spatial Resolution Latitude X Longitude
M1	ACCESS1.0	Commonwealth Scientific Industrial and Research Organization, Bureau of Meteorology Australia	1.25×1.875
M2	BCC-CSM1.1-m	Beijing Climate Center, China	2.8×2.8
M3	CMCC-CMS	Centro Euro-Mediterraneo sui Cambiamenti Climatici Climate Model, Italy	2 x 2
M4	CNRM-CM5[*]	Centre National de Recherches Météorologiques, France	1.4×1.4
M5	GFDL-CM3	Geophysical Fluid Dynamics Laboratory, USA	
M6	HadGEM2-ES	Hadley Centre for Climate Prediction and Research, UK	1.875×1.25
M7	MPI-ESM-LR	Max Planck Institute for Meteorology, Germany	1.80×1.80

3.2. Climate model data

Climate model data used in this study was sourced from the 5th phase of the Coupled Model InterComparison Project (CMIP5) (Taylor et al. 2012). The focus in this study is primarily on the evaluation of the performance of these models in simulating the present-day (1980 – 2005) and future climate projection by mid of the century (2050 – 2075) under two different RCPs (RCP4.5 and RCP8.5). The RCP4.5 is a stabilization scenario, in which the total radiative forcing is stabilized before the end of the present century by the application of a range of technological innovations and policies to reduce greenhouse gas (GHG) and aerosol emissions. On the other hand, the RCP8.5 scenario is considered a business as usual scenario characterized by increasing GHGs and aerosol emissions leading to high concentrations beyond 2100. The labels for the RCPs provide a rough

estimate of the radiative forcing reaching the earth by the year 2100 (relative to preindustrial conditions).

Although there are many models available from CMIP5 that can be used for impact studies, not all models maybe able to simulate key climate processes across all regions of the globe. In this study therefore, we selected CMIP5 models based on the fact that these models have been reported in previous studies by Rowell (2013) and McSweeney et al. (2015) to "realistically" simulate some key climate processes across Africa. These processes include: (i) annual cycles of precipitation and temperature (ii) the West African monsoons and (iii) a minimum of 20 teleconnections in Africa.

Many other studies have also used a sub set of CMIP5 models (Brands et al. 2013; Schewe et al. 2014; Pattnayak et al. 2017; Quesada et al. 2017). The models used in this study together with their spatial resolution and country of origin are shown in Table 1. Monthly precipitation and average temperature from each of the climate models and observed datasets was averaged over the whole basin and for each ecological zone (Sudano, semi-arid and Arid). Analysis were conducted at annual time scale for average temperature and annual and seasonal time scales for precipitation. The seasonal precipitation was averaged for the months of June, July, August and September (monsoon season). The reason for choosing this period was to evaluate the ability of the GCMs models to track the movement of the "tropical rain belt" which some meteorologists suggest is responsible for maximum rainfall in the region (Nicholson 2009; Nicholson 2013; Nicholson 2018) although this assertion remains controversial among tropical meteorologists (Nicholson, 2018).

4. Methodology

The Reliability Ensemble Averaging (REA) technique (Giorgi and Mearns 2002) is based on the assignment of weights to GCMs based on model evaluation. These weights are assigned on the basis of model performance and model convergence. Details of the method are elaborated in the following steps:

Step1: The simple model average method (SMA) whereby the estimated average change in precipitation for all the models is calculated as:

$$\overline{\Delta P} = \frac{1}{N} \sum_{i=1,N} \Delta P_i, \tag{1}$$

233 where N is the total number of models and the overbar indicates the ensemble averaging and ΔP

234 indicates the model-simulated change in precipitation. In the SMA method, all models are given

235 equal weight (One man, One-vote).

236 **Step 2:** The model reliability factor is calculated whereby, the average change, $\widetilde{\Delta P}$, is given by a

237 weighted average of the ensemble members

238

239 $$\widetilde{\Delta P} = \tilde{A}(\Delta P) = \frac{\sum_i^N R_i \Delta P_i}{\sum_i^N R_i},$$ (2)

240

241 where the operator $\tilde{A}$ denotes the REA averaging and R_i is the model reliability factor defined as

242

243 $$R_i = \left[(R_{B,i})^m \times (R_{D,i})^n \right]^{[1/(m \times n)]} = \left\{ \left[\frac{\epsilon_P}{abs(B_{P,i})} \right]^m \left[\frac{\epsilon_P}{abs(D_{P,i})} \right]^n \right\}^{[1/(m \times n)]}$$ (3)

244

245 In Eq (3), R_i is the reliability factor, ϵ is the natural variability (as described in step 5 below). $R_{B,i}$

246 is a factor that measures the model reliability as a function of the model bias ($B_{P,i}$) in simulating the

247 present-day precipitation. It is defined as the difference between the model simulated estimate and

248 observed and the higher the bias, the lower the model reliability. $R_{D,i}$ is a factor that measures the

249 model reliability in terms of the distance ($D_{P,i}$) of the change calculated by a given model from the

250 REA average change, the higher the distance, the lower the model reliability. Therefore, the distance

251 is a measure of the degree of the model convergence of a given model with other ensemble members.

252 In other words, $R_{B,i}$ is a measure of the model performance criterion while $R_{D,i}$ is a measure of the

253 model convergence criterion.

254 **Step 3:** An iterative procedure is used to calculate the distance parameter $D_{P,i}$ starting with an initial

255 guess value as the distance of each ΔP from the ensemble average change $\overline{\Delta P}$, as shown in Eq. (1),

256 i.e. $[D_{P,i}]_1 = [\Delta P_i - \overline{\Delta P}]$. The first guess values are then substituted in Eq. (3) to obtain a first-order

257 REA average change $[\widetilde{\Delta P}]_1$, which is then used to recalculate the distance of each individual model

258 as $[D_{P,i}]_2 = [\Delta P_i - \widetilde{\Delta P}]_1$ and the iteration is repeated until the values converge. According to Giorgi

259 and Mearns (2002), the distance from REA average is only an estimated measure of the model

260 convergence criterion given that the future real conditions are not known.

Step 4: The parameter m and n in Eq. (3) can be used to weigh each criterion. In this study m and n are assumed to be 1, giving equal weight to both criteria. $R_{B,i}$ and $D_{P,i}$ are set to 1 when B and D are smaller than $\in_P$, respectively. Thus Eq. (3) states that the model projection is considered "reliable" when both its bias and distance from the ensemble average are within the natural variability $\in$, so that $R_B = D_{P,} = 1$. As the bias and/or distance grow, the reliability of a given model simulation decreases.

Step 5: The parameter $\in_P$ in Eq. (3) is a measure of natural variability in the 30-year average annual or seasonal precipitation and temperature. To calculate $\in$ in this study, the time series of observed monthly precipitation and average temperature covering the period 1901 – 2005 obtained from CRU were employed. Then, 30-year moving averages of the series are calculated after linearly detrending the data (to remove century-scale trends), and $\in$ estimated as the difference between the maximum and minimum values of these 30-year moving averages. Natural variability in rainfall and average temperature was calculated only for the whole basin.

Step 6: In order to calculate the uncertainty range around the REA average change, the REA root mean square difference (rmsd) of the changes $\tilde{\delta}_{\Delta P}$, has to be obtained and is defined by

$$\tilde{\delta}_{\Delta P} = \left[\tilde{A}\left(\Delta P_i - \widetilde{\Delta P}\right)^2\right]^{1/2} = \left[\frac{\sum_i R_i\left(\Delta P_i - \widetilde{\Delta P}\right)^2}{\sum_i R_i}\right]^{1/2} \tag{4}$$

The upper and lower uncertainty limits are defined as

$$\Delta P_+ = \widetilde{\Delta P} + \tilde{\delta}_{\Delta P} \tag{5a}$$
$$\Delta P_- = \widetilde{\Delta P} - \tilde{\delta}_{\Delta P} \tag{5b}$$

The total uncertainty range is then given by $\Delta P_+ - \Delta P_- = 2\tilde{\delta}_{\Delta P}$. According to the REA method, when the changes are distributed following a Gaussian PDF, the rmsd is equivalent to the standard deviation so that the $\mp\delta$ range would imply a 68.3% confidence interval. For a uniform PDF, that is, one in which each change has the same probability of occurrence, the $\mp\delta$ range implies a confidence interval of about 58%. Moreover, in the REA method, the normalized reliability factors of Eq. (3) are interpreted as the likelihood of a GCM outcome, meaning that; the greater the factor,

290 the greater the likelihood associated with the model simulation. In this study the analysis was carried

291 out for the whole basin and for each of the ecological regions.

292 >>>>>>>>>>>>>>>>>>**Figure 4**>>>>>>>>>>>>>>>>>>>>

Figure 4: Annual precipitation cycle (a) over the Lake Chad basin, (b) over the Sudano zone, (c) over the semi-arid zone, (d) over the arid zone.

5. Results

5.1. Historical precipitation

300   Evaluation of historical precipitation over the LCB indicate that all CMIP5 models used in

301 this study were able to replicate the annual precipitation cycle over the basin and at the level of

302 different ecological zones (Figure 4). A strong feature of rainfall over the LCB is its unimodal cycle

303 which follows the north – south seasonal migration of the tropical rain belt. Most models were able

304 to capture this feature satisfactorily at basin scale. Despite this, some models appear to be bimodal

305 or have very broad peak (e.g. M2 has a peak of 6 months) as opposed to 3 months in observations.

306 Furthermore, across the basin, most models overestimate dry season rainfall and all but two

307 underestimate wet season rainfall (M2 and M5) (Figure 4a).

308   It was also observed across the basin that, there was a large spread among models in monthly

309 precipitation estimates during the dry season compared to other months (Figure 3). Overall seasonal

310 precipitation was more variable in the semi-arid zone (75 – 235 mm) compared to the Sudano zone

12

311 (160 – 240 mm). Furthermore, the MME monthly mean precipitation estimates were consistently

312 lower than estimates from CRU and WFDEI across the basin and at the level of the ecological zones

313 (Figure 4).

314   Agreement in observed and simulated monthly precipitation was also evaluated using Taylor

315 diagram (Figure 5a). In the polar plot, the reference or observed data are plotted on the x-axis

316 (abscissa), and the model-simulated values are expected to lie in the first quadrant if the correlation

317 coefficient is positive. The radial dimension indicate the normalized standard deviation (calculated

318 as the ratio of standard deviation of simulated over standard deviation of observed, ratios >1 indicate

319 that the simulated values are more variable than observed), and the angular dimension shows the

320 correlations. These statistics were computed using the 1980 – 2005 monthly precipitation. The

321 similarity between model-simulated and observed precipitation is quantified in terms of their

322 correlation and the amplitude of the variability. The correlation coefficients between each model and

323 the monthly observations from CRU are in the range 0.50 – 0.95 and between the MME and

324 observation is 0.85. This indicates that there are strong correlations between the estimates from the

325 models and CRU. The strong correlation value between MME and CRU indicate that the MME

326 performs slightly better than some individual GCM models (M1, M2, M3, M5, and M6). Models

327 M4 and M7 show large variability compared to other models with normalized standard deviation >1

328 although both models have high correlation coefficients >0.85.

329

330 Table 2: Model simulated biases of present-day precipitation (%) and average temperature (°C)

| Time scale	Ecological Zone	GCM							
		M1	M2	M3	M4	M5	M6	M7	MME
Annual precipitation	LCB	12.11	13.39	-11.71	59.16	30.20	7.08	27.28	19.65
	Sudano	21.81	20.21	25.78	39.73	17.15	11.89	38.36	24.99
	Semi-arid	-6.07	-20.86	-33.70	82.14	17.31	-3.61	22.78	8.28
	Arid	-51.86	-59.17	-82.19	48.37	27.35	-38.63	2.80	-21.90
Monsoon (JJAS) precipitation	LCB	-26.08	-41.14	-32.77	35.51	-12.65	-22.88	9.24	-12.97
	Sudano	-8.16	-20.93	-3.93	20.55	-9.30	-11.10	13.61	-2.75
	Semi-arid	-28.31	-48.72	-40.38	57.59	-18.31	-23.04	12.41	-12.68
	Arid	-62.74	-73.90	-84.99	31.77	-10.58	-49.22	-6.02	-36.52
Annual average temperature	LCB	-2.98	-2.31	-2.96	-6.03	-4.37	-4.69	-3.85	-3.88
	Sudano	-2.30	-2.17	-3.27	-4.99	-4.68	-3.75	-4.22	-3.62
	Semi-arid	-2.80	-2.33	-2.35	-6.79	-4.28	-4.80	-4.25	-3.94
	Arid	-3.83	-2.42	-3.25	-6.33	-4.16	-5.52	-3.09	-4.09

331

332   As a first step to quantify uncertainty using the REA method, the model performance criteria

333 based on its ability to simulate the present-day climate was assessed using the bias factor. At the

annual time-scale the GCMs produced mostly positive biases in the range 7 – 60% of the observed precipitation and only M3 produced a negative bias (-11%) (Table 2) indicating that, most of the models have a wet bias. At the level of ecological zones, all the models overestimated annual precipitation in the Sudano zone in the range 10 – 40% of observed (wet bias). The results are mixed in the other ecological zones ranging between -30 – 80% in the semi-arid and -80 – 50% in the arid zone (Table 2). At the seasonal time-scale, the GCMs mostly underestimated monsoon precipitation (JJAS) over the whole basin and the level of the ecological zones except M4 and M7 (Table 2) indicating a dry bias in the monsoon season.

>>>>>>>>>>>>>>>>>>>>**Insert Figure 5**>>>>>>>>>>>>>>>>>>>>>>>>>>>>>>>>

Figure 5: Taylor diagram showing comparison of monthly (a) precipitation, (b) average temperature simulated over the LCB with observations using CRU for the period 1980 – 2005

5.2. Historical temperature

The results of historical annual average temperature cycle over the LCB were quite varied among the CMIP5 models with only M1, M4 and M7 accurately reproducing the temperature cycle with maximum average temperature observed in April and minimum in August. Most of the models underestimate average temperature in April and systematically overestimated it in August with the exception of M4 and M5. This is consistent with too much rainfall in April (causing a cooling) and too little rainfall in August (Figure 6).

The simulation of present-day average temperature over the basin was further evaluated using the Taylor diagram (Figure 5b). The correlations between the observed and simulated monthly

temperature was in the range 0.40 – 0.90. However, most GCMs show large variability with normalized standard deviations >1 (M1, M3, M5, M6, M7). Four models produced correlation coefficients >0.75 which could be considered as strong. Meanwhile, the MME produced a correlation coefficient of 0.86 stronger than what was obtained for some individual models (M2, M5, and M6).

The model performance criteria based on its ability to simulate the present-day climate was also assessed using the bias factor. At the annual time-scale all the GCMs produced negative biases, underestimating present-day average temperature throughout the LCB and at the level of the different ecological zones indicating a generalized cold bias. Average temperature was underestimated in the range of (-2℃) – (-6°C) (Table 2). These results are contrasting with those of precipitation whereby varied results showing both positive and negative biases were obtained.
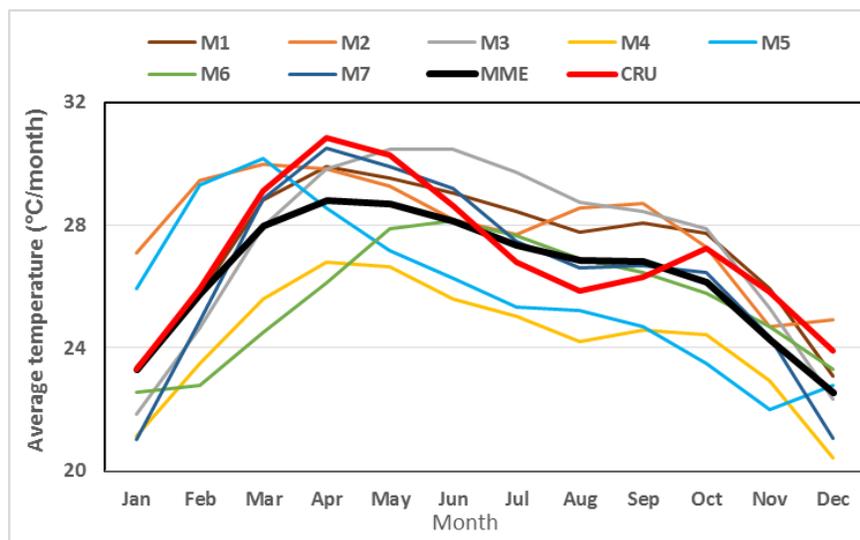
Figure 6: Annual temperature cycle over the Lake Chad basin

5.3. Future annual precipitation projections in the LCB (2050 – 2075)

Analysis using the REA technique indicate that, future annual precipitation in the LCB is projected to increase by about 2.5% across the basin under the RCP4.5 scenario relative to the historical period (1980 – 2005). At the level of the different ecological zones, future annual precipitation is projected to increase by 22% in the Sudano zone, 4% in the semi-arid and a decline of about -12% in the arid zone relative to the historical period. Under the RCP8.5 scenario, future annual precipitation is projected to increase by about 5% across the LCB which is double the RCP4.5 scenario. These results corroborate the findings of Aloysius et al. (2016) in the Central Africa region

covering the LCB whereby, the authors also projected an increase in precipitation in the region from an ensemble of CMIP5 models by the end of the present century. At the level of ecological zones, projections for future annual precipitation is projected to increase by 30%, 9% and 5% for the Sudano, semi-arid and arid zones respectively. Under the RCP8.5 scenario, the Sudano zone show an increase of about 8% higher than the projection from RCP4.5 scenario while the arid zone may experience a drop of about of about -5% relative to the historical period (Table 3 and Figure 7).
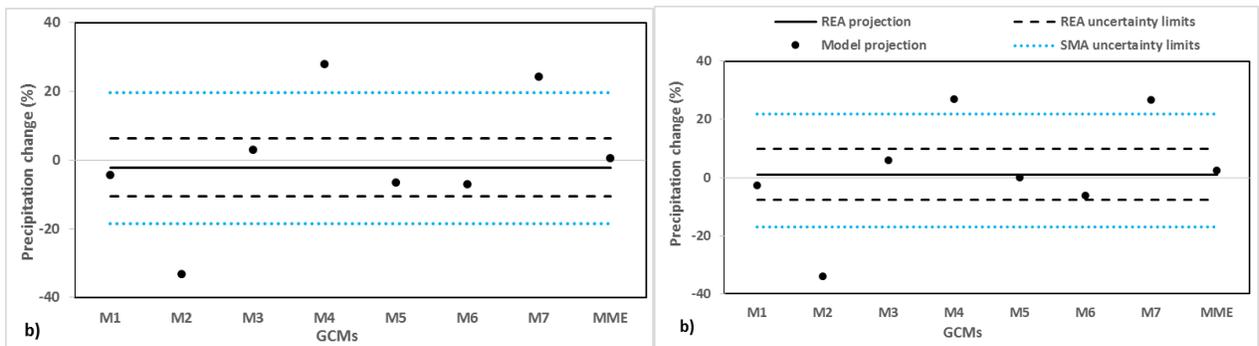
388
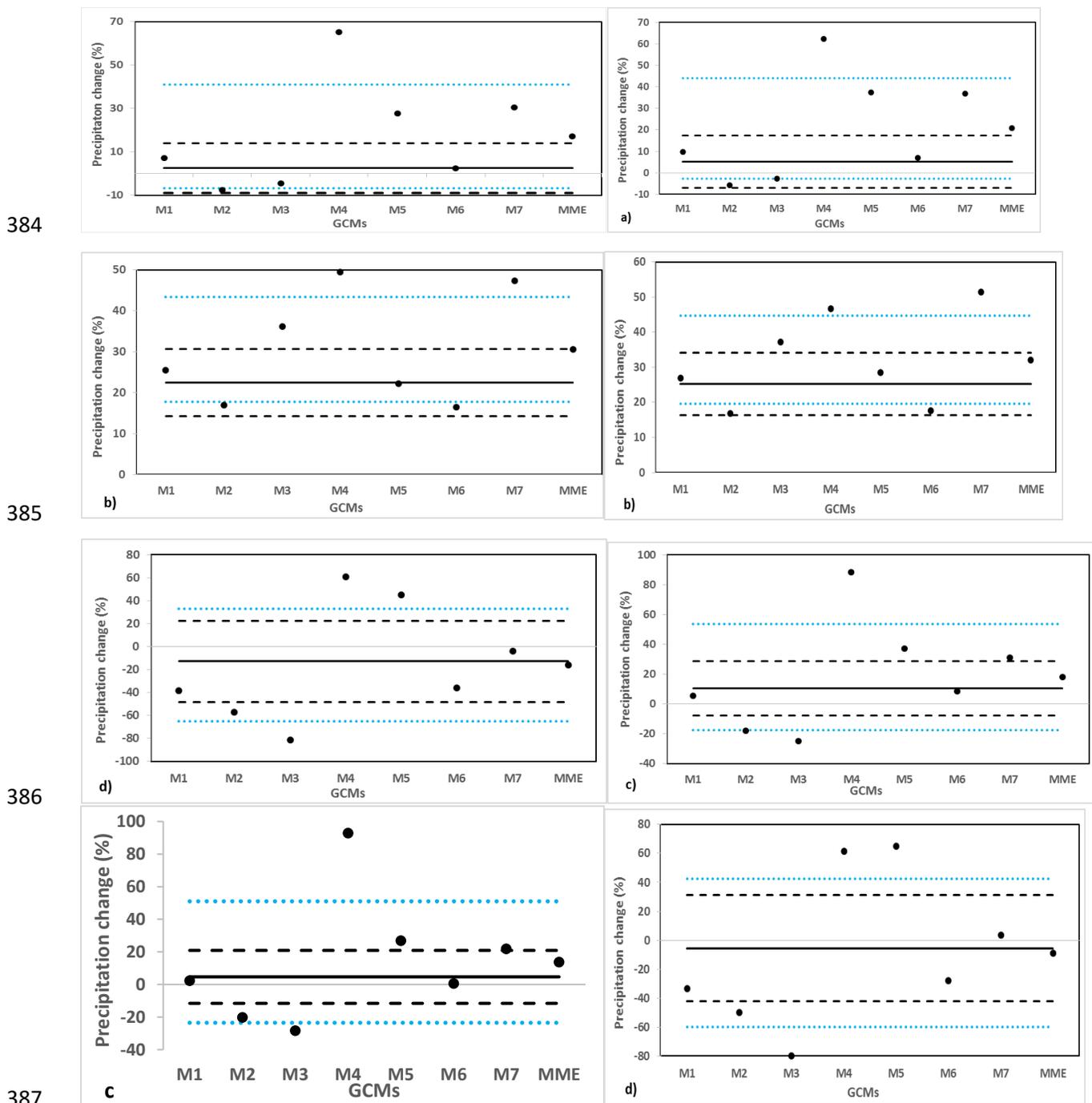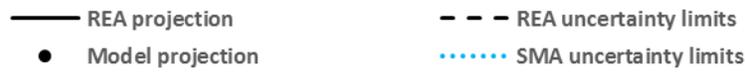
Figure 7: Annual precipitation projection under RCP4.5 (first column) and RCP8.5 (second column) a – d represents the LCB, sudano, semi-arid and arid zones respectively

Monsoon precipitation is projected to decrease across the basin by -11% and 5% under the RCP4.5 and RCP8.5 respectively. At the level of the different ecological zones monsoon precipitation is also projected to decrease across all the ecological zones and for both scenarios under investigation (Table 3 and Figure 8).
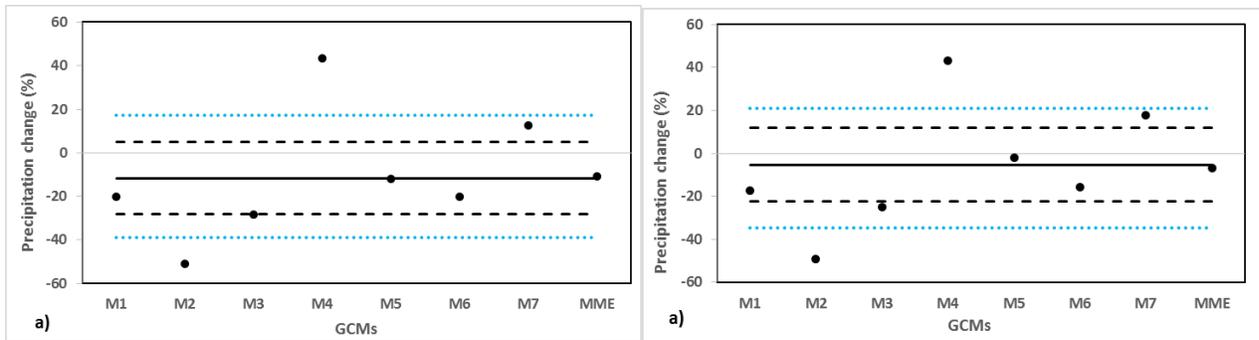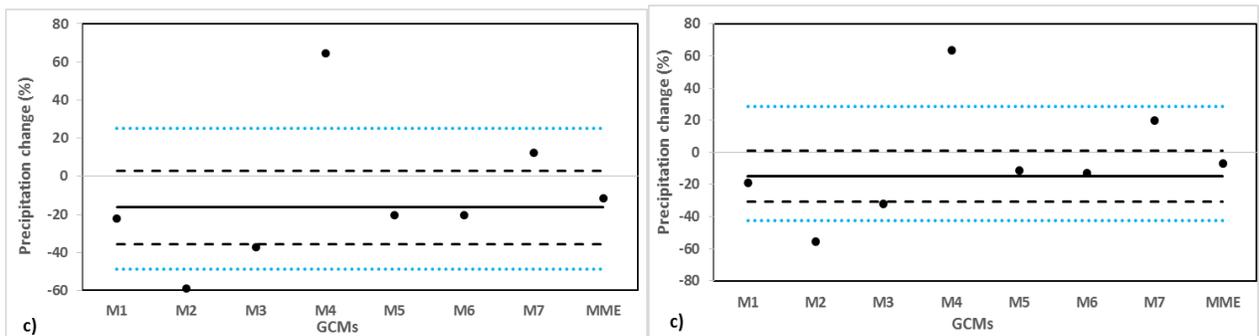
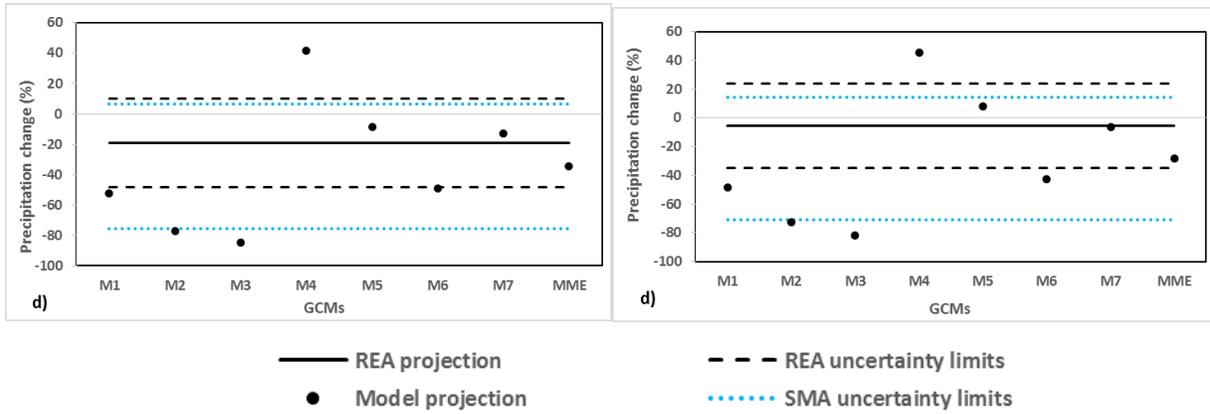Figure 8: Seasonal precipitation projection under RCP4.5 (first column) and RCP8.5 (second column), a – d represents the LCB, sudano, semi-arid and arid zones respectively

Regarding the uncertainties in future precipitation projections, the REA average changes are all within the range of natural variability ϵ_P across the LCB under the two concentration pathways RCP4.5 and RCP8.5 (Table 3). Although this does not discount the fact that the changes in future precipitation are not statistically significant. At the level of the different ecological zones, the uncertainty range is also in the same order of magnitude with the natural variability although there is an increase of more than 10% in the arid zone. Comparing the three different ecological zones together, uncertainty is lower in the Sudano zone while the arid zone displays the highest level of uncertainty which follows the same trend that was observed for natural variability (Table 3).

Considering projections from individual CMIP5 models, under the RCP4.5 scenario, M1, M4, M5, M6, and M7 project an increase in future annual precipitation while M2, and M3 project a decrease at the basin scale. M1 M2, M3 and M6 lie within the uncertainty range but only M1 and M6 project and increase while M2 and M3 project a decrease (Figure 7a). The results are varied for the different ecological zones. In the Sudano zone, all models project an increase in future annual precipitation with M1, M2, M5, and M6 lying within the uncertainty range (Figure 7b). Within the semi-arid zone, all models project an increase in future precipitation except M2 and M3, although only projections from M1, M6 and M7 fall within the uncertainty range (Figure 7c). In the arid zone only M4 and M5 project an increase in future precipitation although their results are outside the uncertainty range while the rest project a decrease. (Figure 7d).

Under the RCP4.5 scenario, M4 and M7 project an increase in future monsoon precipitation while the other models project a decrease at basin scale with results lying outside the uncertainty range (not shown). In the Sudano zone, M3, M4 and M7 project an increase in future monsoon

18

precipitation while the other models project a decrease although only projections from M3 lie within the uncertainty range (not shown). Results in the semi-arid zone are similar to those obtained in the Sudano zone. In the arid zone, only M4 project an increase in future monsoon precipitation while the rest of models project a decrease however and results do not lie within the uncertainty range (not shown).

Under the RCP8.5 scenario, future annual precipitation is projected to increase across the LCB by all models except M2 and M3 with projections from M1 and M6 lying within the uncertainty range (Figure 7a). In the Sudano zone, all models project an increase in future annual precipitation with projections from M1, M2, M5 and M6 lying within the uncertainty range (Figure 8b). In the semi-arid zone, all models except M2 and M3 project an increase with projections from M1 and M6 lying within the uncertainty range (Figure 7c). Model M4, M5 and M7 project an increase in the arid zone while the other models project a decrease with projections from M7 lying within the uncertainty range. Individual model projections for monsoon precipitation under this scenario are similar to what was obtained under the RCP4.5 scenario although with different magnitudes (not shown).

Table 3: Natural variability, projected precipitation change and uncertainty range

Time scale	Ecological zone	Natural variability (εP) (mm)	RCP4.5		RCP8.5	
			ΔP (%)	Uncertainty ($\pm\delta\Delta P$)	ΔP (%)	Uncertainty ($\pm\delta\Delta P$)
Annual precipitation	LCB	84.40 (11.43)	2.54	11.37	5.26	12.13
	Sudano	81.81 (7.24)	22.61	8.29	30.56	8.97
	Semi-arid	95.23 (11.89)	4.15	15.69	9.72	16.92
	Arid	88.33 (23.15)	-12.32	34.77	-4.77	36.34
Monsoon precipitation	LCB	16.45 (11.32)	-11.61	16.52	-5.29	17.11
	Sudano	12.68 (6.38)	-0.72	12.55	3.14	12.39
	Semi-arid	21.59 (14.44)	-16.63	18.39	-9.28	18.58
	Arid	20.75 (23.59)	-23.11	25.49	-13.79	28.35

*The values in bracket represent the percentage change in precipitation relative to the historical period (1980 – 2005)

5.4. Future average temperature projections in the LCB (2050 – 2075)

Analysis using the REA technique show that future annual average temperature across the LCB under the RCP4.5 and RCP8.5 scenarios is projected to decrease by about 1°C relative to the historical period (1980-2005) and by almost the same amount across the different ecological zones (Table 4). These results are quite contrasting to what has been observed globally from CMIP5 models which generally project an increase in future global average temperatures (Knutti and Sedláček 2013) and in the African continent (Dike et al. 2015).

451   Regarding uncertainty in the future annual average temperature projections, the REA average

452 changes are outside the range of natural variability $\in_T$ across the LCB and at the level of the different

453 ecological zones under both RCPs. Natural variability in annual average temperature is highest in

454 the arid zone and lowest in the Sudano zone. However, uncertainty in model projections of annual

455 average temperature is highest in the semi-arid zone and lowest in the arid zone (Figure 9).

456   Considering future projections from individual CMIP5 models, under the RCP4.5 scenario,

457 only M1 consistently projects an increase in future annual average temperature over the LCB and at

458 the level of different ecological zones while all the other models project a decrease (Figure 8). Under

459 the RCP8.5 scenario, M1 and M3 consistently project an increase in projected future annual

460 temperature over the basin and at the level of the Sudano and semi-arid zones while only M3 project

461 an increase in the arid zone. The projections from models showing an increase in future average

462 temperature all lie outside the uncertainty range while the results are mixed for those projecting a
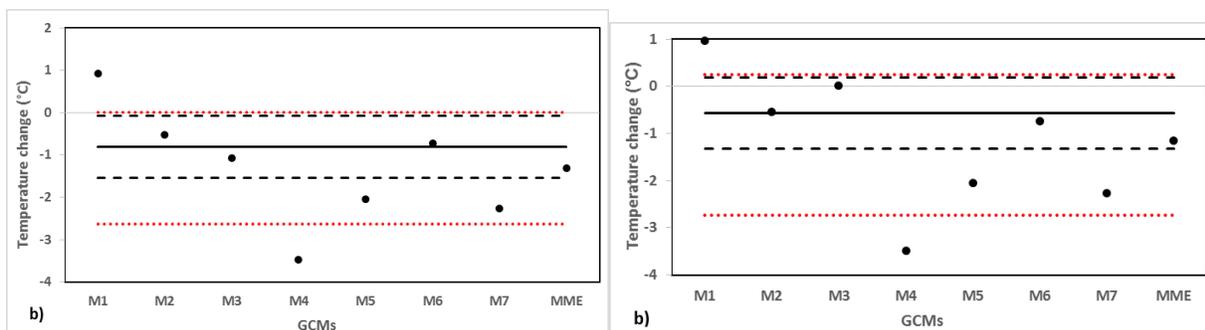
463 decrease (Figure 9).

464 Table 4: Natural variability, projected temperature change and uncertainty range

Time scale	Ecological zone	Natural variability (εT) (°C)	RCP4.5		RCP8.5	
			ΔT (°C)	Uncertainty ($\pm\delta\Delta T$)	ΔT (°C)	Uncertainty ($\pm\delta\Delta T$)
Annual average temperature	LCB	0.50	-1.02	0.89	-0.99	0.98
	Sudano	0.28	-0.84	0.78	-0.55	0.90
	Semi-arid	0.48	-0.70	1.04	-0.70	1.19
	Arid	0.68	-0.85	0.72	-0.72	0.79

465

466 a)

467 b)
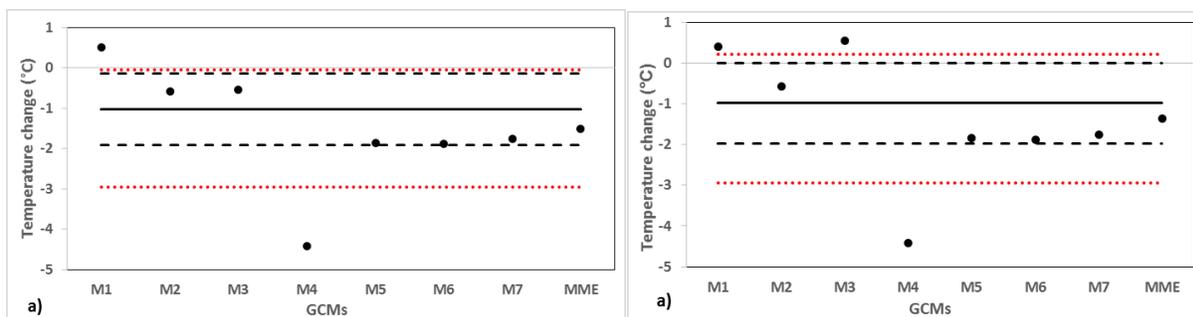
468
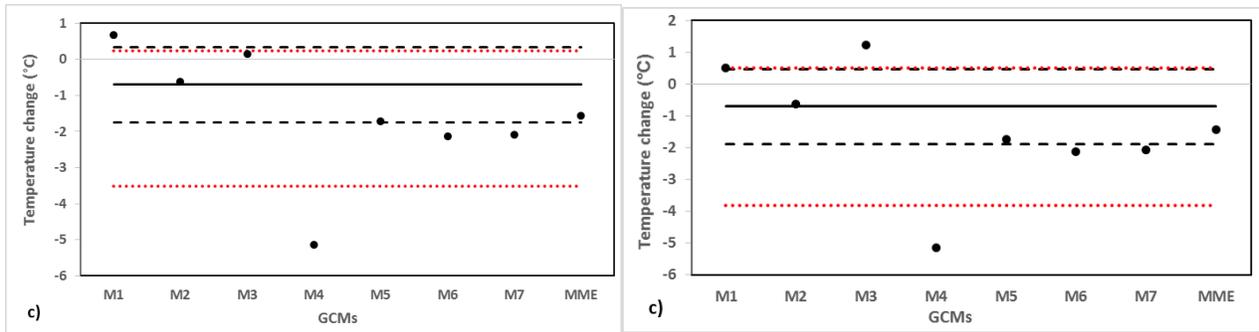
469
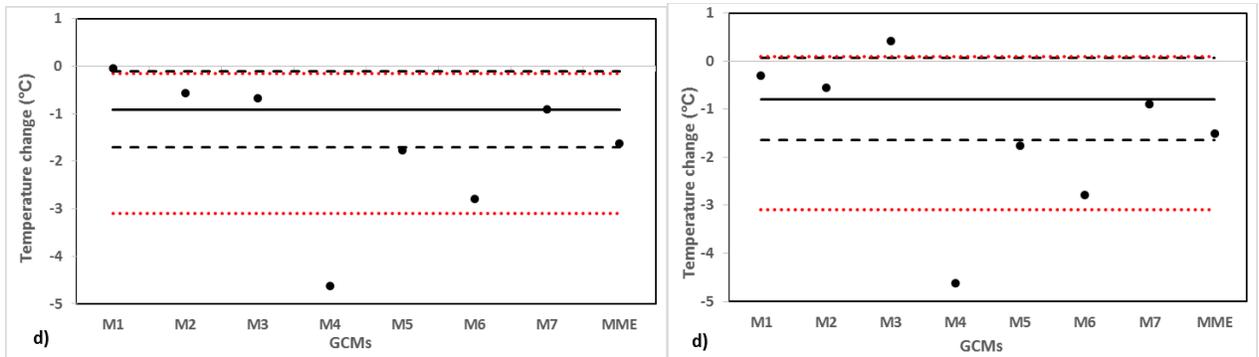
470

REA projection — — — REA uncertainty limits

● Model projection ••••••• SMA uncertainty limits

Figure 9: Annual average temperature projection under RCP4.5 (first column) and RCP8.5 (second column) a – d represents the LCB, sudano, semi-arid and arid zones respectively

5.5. Reliability analysis of CMIP5 models for precipitation and temperature projections

Under RCP4.5 and RCP8.5, M1, M2, M3 and M6 produced model reliability factors ≥0.85 for future annual precipitation projection in the LCB and all projections from these models lie within the REA uncertainty range (Figure 7a). This performance can be attributed to the fact that, (i) the bias factor (difference between the model simulated estimate and observed), and under both RCPs (ii) the convergence factor (distance between the model projection and REA average) for each of the models are within the bounds of natural variability $\in_P$. Models with low reliability factors equally produced low bias and convergence factors (Table 5) and projections from these models all lie outside the REA uncertainty range (Figure 7a).

At the seasonal scale only M5 produced a reliability factor >0.80 and the projection from this model is very close to the REA average. The low performance of the CMIP5 models for monsoon projection can be attributed to the fact that apart from M5 and M7, most of the models produced very low bias factors mostly below 0.5 as a result of their consistent underestimation of monsoon

21

488 precipitation relative to the historical period. It can also be observed that even though M1, M3, and

489 M6 produced very high convergence factors for projected monsoon precipitation, these models were

490 penalized because of their low bias factors. On the other hand, M7 which produced a high bias factor

491 for monsoon precipitation was penalized because of its low convergence factor (Table 5). By given

492 equal weights to criteria m and n in Eq. (3) any model which performs well in one criteria and does

493 not equally perform well in the other is penalized.

494 The reliability factors of the various models for annual average temperature projection in the

495 LCB under RCP4.5 and RCP8.5 scenarios are generally very low with some values <0.10. This low

496 performance can be attributed to the inability of the models to simulate historical annual average

497 temperature resulting in a generalized low bias factors among the CMIP5 models. Even though all

498 models except M1 and M4 under the RCP4.5 scenario and M2, M5, M6 and M7 under the RCP8.5

499 scenario produced high convergence factors, these models were penalized because of their low

500 ability to simulate historical average temperature.

501 Comparing the results from REA average and simple model average (SMA) or MME for

502 annual and seasonal precipitation projections, it was observed that, under the two RCPs, estimates

503 from SMA (MME) do not deviate significantly from the REA average and in most cases lie within

504 the REA uncertainty range (Figures 7 - 8). This shows that both methods produce ensemble averages

505 that are similar in magnitude. This is an interesting finding given that each model received a different

506 weight through the application of either techniques. In the SMA (MME) technique, each model

507 received the same weight while with REA technique the weight attached to each model was based

508 on its reliability factor which was determined by both the bias and convergence factors. Previous

509 studies have also shown that both methods produced similar results e.g. (Miao et al. 2014; Mani and

510 Tsai 2016). However, it can also be observed from the figures that the uncertainty range for SMA is

511 larger than that of REA technique

512

513

514

515

516

517

518

519

520 Table 5 Model performance for historical and future projections for annual and monsoon precipitation

Model	Annual precipitation					Monsoon precipitation				
	Bias factor	RCP 45		RCP 85		Bias factor	RCP 45		RCP 85	
		Convergence factor	Reliability factor	Convergence factor	Reliability factor		Convergence factor	Reliability factor	Convergence factor	Reliability factor
M1-ACCESS1.0	0.94	1.00	0.94	1.00	0.94	0.43	1.00	0.43	0.96	0.42
M2-bcc_ESM1-1-M	0.85	1.00	0.85	1.00	0.85	0.28	0.29	0.08	0.26	0.07
M3-CMCC_CMS	0.98	1.00	0.98	1.00	0.98	0.35	0.66	0.23	0.59	0.20
M4-CNRM-CM5	0.19	0.18	0.04	0.20	0.04	0.32	0.21	0.07	0.23	0.07
M5-GFDL-CM	0.38	0.46	0.17	0.36	0.13	0.89	1.00	0.89	1.00	0.89
M6-HadGEM-ES	1.00	1.00	1.00	1.00	1.00	0.49	1.00	0.49	1.00	0.49
M7-MPI-ESM-LR	0.42	0.41	0.17	0.36	0.15	1.00	0.47	0.47	0.48	0.48

521 *Note that the different ecological zones are not considered

522

6. Discussion

Given the fact that some models showed systematic biases in the seasonal rainfall estimates indicate that they were not able to tract the north-south displacement of the ITCZ as they are consistently too wet in the dry season, and too dry in the wet season.

The fact that MME (SMA) produced stronger correlations compared to some individual models in the Taylor diagram for both precipitation and average temperature can be attributed to the fact that, by averaging all the models together, the individual model biases cancel out thus resulting to an ensemble that outperforms some of the individual CMIP5 models.

Even though the CMIP5 models used in this study were reported to simulate some key climate processes in the region based on the findings of Rowell (2013) and McSweeney et al. (2015), results from our study show that, there was still a large spread in the model output which can be attributed to individual model physics. Despite this spread, most of the models were able to replicate the historical annual rainfall cycle across the basin and at the level of the different ecological zones indicating some level of objectivity in the selection process. Furthermore, the ensemble projections from the MME (SMA) average were mostly within the bounds of uncertainty limits across the basin and at the level of the ecological zone which can also be attributed to the model selection process.

Apart from biases associated with model physics, biases in the model simulations could also be attributed to the inability of the individual CMIP5 model to simulate other local scale atmospheric processes and mesoscale convective systems (MCSs) and non-climatic effects like orography that also influence climate in the region (Nkiaka et al., 2017c). This is largely due to their coarse spatial resolutions. In fact, MCSs are difficult to be modelled because these events organize dynamically on spatial scales that cannot be resolved by the current generation of GCMs (Taylor et al. 2017). Other mechanisms that influence regional climate in LCB include the low level Bodele Jets (Washington et al. 2006), the high level Tropical Easterly Jets (TEJ) and the West African Westerly Jets (WAWJ) which are stronger in the eastern Sahel where the LCB is located (Nicholson 2013) and the high level African Easterly Jet (AEJ) which influence precipitation over the Central African region (Farnsworth et al. 2011). It is not known how these jet streams are simulated in the CMIP5 models although their influence on regional rainfall is very significant (Nicholson et al., 2013).

Despite the poor performance of the GCMs to continuously underestimate historical monsoon precipitation in this study, previous studies also reported the decline in monsoon

precipitation in the region (Polson et al. 2014; Nkiaka et al. 2017b) albeit causes of this decline are not yet well understood. Nevertheless, Devaraju et al. (2015) attributed it to large scale deforestation in the northern middle and high latitudes which force the ITCZ to shift southwards resulting in a significant decrease in monsoon precipitation. Quesada et al. (2017) also attributed the decline in monsoon precipitation in historical and future climate projections to biophysical effects of large scale land use/cover changes. Despite this, recent studies by Taylor et al. (2017) have shown that, extreme precipitation events from MCSs during the monsoon season has increased in the region. Nonetheless the study by Taylor et al. (2017) did not mention the contribution of MCSs extreme precipitation events to the total monsoon precipitation although their contribution to total annual precipitation in that study was estimated to be < 25%.

Generally, results from this study show an increase in projected annual precipitation by mid of the century with five models projecting this increase under both RCPs. These results are also supported by the MME (SMA) average whereby equal weights are attached to each model and REA average whereby weights are attached to a model based on the model reliability factor. In each case, future annual precipitation is projected to increase in the LCB. At the level of the different ecological zones, all models project an increase in future precipitation in the Sudano, five models project an increase in the semi-arid and three models project an increase in the arid zone under both RCPs.

Another significant finding from this study is the fact that, although CMIP5 models project a decrease in future monsoon precipitation which is known to contribute to most of the rainfall in the region, overall, annual precipitation is still projected to increase by the middle of the century under both RCPs. This implies that in future, the seasonal north – south migration of the ITCZ which brings monsoon precipitation into the region may no longer be the dominant mechanism responsible for rainfall in the region. This is consistent with other studies in the region that have reported of a dryer onset of the monsoon season and an intensification of the late rainy season (Biasutti 2013). Another study by Monerie et al. (2016) has also reported of an increase in late rainy season (September and October) rainfall and a delay in the retreat of the monsoon. This can partly explain why even though the CMIP5 models are projecting a decrease in monsoon precipitation, annual precipitation is still projected to increase across the LCB.

The increase in projected annual precipitation in the region under climate change have been attributed to many reasons e.g. Dong and Sutton (2015) attribute it to the rising levels of GHGs in the atmosphere, Evan et al. (2015) attribute it to an upward trend in the Sahara heat low (SHL) temperature resulting from atmospheric greenhouse warming by water vapor. In separate studies,

586 Biasutti (2013) and Park et al. (2015) attributed the increase in future precipitation in the region as
587 projected by CMIP5 models to increased moisture convergence in the region under climate change.
588 Generally, the models were biased in simulating historical and future projected average temperature
589 in the LCB. The poor performance by GCMs in simulating average surface temperature in this study
590 may be attributed to increased insolation over region considering that the region is known to be one
591 of the cloudiest in the tropics; it could also be attributed to large biases in GCMs in simulating cloud
592 climatology (Lauer and Hamilton 2013; Diallo et al. 2014; Dommo et al. 2018).

7. Conclusion

594 The objectives of this study were to evaluate the ability of CMIP5 models to reproduce the
595 present-day climate conditions in the LCB (1980-2005), assess the future climate projections for the
596 basin by the middle of century (2050 – 2075) relative to the historical period and quantify the
597 uncertainties associated with these projections using two Representative Concentration Pathways
598 (RCP4.5 and 8.5). This is the first study that uses climate models to assess future precipitation and
599 average temperature projections in the LCB. Results indicate an increase in precipitation across the
600 study domain under RCP4.5 and RCP8.5 by mid of the century, with the Sudano zone expected to
601 experience the highest amount of future annual precipitation.

602 Results further indicate that, the CMIP5 models simulated precipitation better than
603 temperature as a result of a cold bias observed in the simulation of annual average temperature by
604 the models. Although results from the study vary from one model to another, overall M4 performed
605 poorly as it consistently overestimated future projected precipitation and underestimated annual
606 average temperature across the basin and at the level of the different ecological zones under both
607 RCPs. In addition, no projections from this model lie within the uncertainty range suggesting that,
608 M4 is an outlier within the ensemble used in this study and may not be recommended for future
609 impact studies in the LCB. For impact studies in the LCB using CMIP5 models, M1 and M6 with
610 future precipitation projections that consistently lie within the REA uncertainty limits under both
611 RCPs may be recommended. Meanwhile M1 which projected increasing temperature trends in
612 agreement with global and continental trends may be recommended for impact studies in the basin.
613 Overall M1 will be suitable for hydrological modelling studies in the LCB.

614 Results from this study also show that the REA technique which uses a reliability factor
615 whereby weights are attached to a model based on its ability to simulate both the present-day climate
616 through the bias factor and future climate through the convergence factor is a robust method to

26

considerably reduce uncertainties in climate models to compared to the Simple model averaging (SMA) technique. The weights attached to each model is calculated based on past natural climate variability observed in the area. Using this approach, uncertainty limits obtained in this study especially for precipitation were mostly within the bounds of natural rainfall variability across the LCB.

Nevertheless, biases observed in the models could be reduced and results obtained in this study refined by using regional climate models. Results could also be fine – tuned in future as high resolution GCMs become available.

Acknowledgements

References

ADENLE, D. 2001. *Groundwater resources and environmental management in Niger Basin Authority and Lake Chad Basin Commission agreements*. UIPO, Ibadan, Nigeria.

AKURUT, M., P. WILLEMS and C. NIWAGABA. 2014. Potential Impacts of Climate Change on Precipitation over Lake Victoria, East Africa, in the 21st Century. *Water,* **6**(9), p2634.

ALOYSIUS, N. R., J. SHEFFIELD, J. E. SAIERS, H. LI and E. F. WOOD. 2016. Evaluation of historical and future simulations of precipitation and temperature in central Africa from CMIP5 climate models. *Journal of Geophysical Research: Atmospheres,* **121**(1), pp.130-152.

ARMITAGE, S. J., C. S. BRISTOW and N. A. DRAKE. 2015. West African monsoon dynamics inferred from abrupt fluctuations of Lake Mega-Chad. *Proceedings of the National Academy of Sciences,* **112**(28), pp.8543-8548.

ARNELL, N. W. 2004. Climate change and global water resources: SRES emissions and socio-economic scenarios. *Global environmental change,* **14**(1), pp.31-52.

BIASUTTI, M. 2013. Forced Sahel rainfall trends in the CMIP5 archive. *Journal of Geophysical Research: Atmospheres,* **118**(4), pp.1613-1623.

BRANDS, S., S. HERRERA, J. FERNÁNDEZ and J. M. GUTIÉRREZ. 2013. How well do CMIP5 Earth System Models simulate present climate conditions in Europe and Africa? *Climate dynamics,* **41**(3-4), pp.803-817.

DEVARAJU, N., G. BALA and A. MODAK. 2015. Effects of large-scale deforestation on precipitation in the monsoon regions: Remote versus local effects. *Proceedings of the National Academy of Sciences,* **112**(11), pp.3257-3262.

654 DIALLO, I., C. L. BAIN, A. T. GAYE, W. MOUFOUMA-OKIA, C. NIANG, M. D. DIENG and R. GRAHAM. 2014.
655   Simulation of the West African monsoon onset using the HadGEM3-RA regional climate model.
656   *Climate dynamics,* **43**(3-4), pp.575-594.

657 DIKE, V. N., M. H. SHIMIZU, M. DIALLO, Z. LIN, O. K. NWOFOR and T. C. CHINEKE. 2015. Modelling present
658   and future African climate using CMIP5 scenarios in HadGEM2-ES. *International Journal of*
659   *Climatology,* **35**(8), pp.1784-1799.

660 DOMMO, A., N. PHILIPPON, D. A. VONDOU, G. SÈZE and R. EASTMAN. 2018. The June-September low cloud
661   cover in Western Central Africa: mean spatial distribution and diurnal evolution, and associated
662   atmospheric dynamics. *Journal of Climate,* (2018).

663 DONG, B. and R. SUTTON. 2015. Dominant role of greenhouse-gas forcing in the recovery of Sahel rainfall.
664   *Nature Climate Change,* **5**(8), pp.757-760.

665 EVAN, A. T., C. FLAMANT, C. LAVAYSSE, C. KOCHA and A. SACI. 2015. Water vapor–forced greenhouse
666   warming over the Sahara Desert and the recent recovery from the Sahelian drought. *Journal of*
667   *Climate,* **28**(1), pp.108-123.

668 FARNSWORTH, A., E. WHITE, C. J. R. WILLIAMS, E. BLACK and D. R. KNIVETON. 2011. Understanding the
669   Large Scale Driving Mechanisms of Rainfall Variability over Central Africa. *In:* C. J. R. WILLIAMS and
670   D. R. KNIVETON, eds. *African Climate and Climate Change: Physical, Social and Political Perspectives.*
671   Dordrecht: Springer Netherlands, pp.101-122.

672 FOTSO-NGUEMO, T. C., D. A. VONDOU, C. TCHAWOUA and A. HAENSLER. 2017. Assessment of simulated
673   rainfall and temperature from the regional climate model REMO and future changes over Central
674   Africa. *Climate dynamics,* **48**(11-12), pp.3685-3705.

675 GIORGI, F. and L. O. MEARNS. 2002. Calculation of average, uncertainty range, and reliability of regional
676   climate changes from AOGCM simulations via the "reliability ensemble averaging"(REA) method.
677   *Journal of Climate,* **15**(10), pp.1141-1158.

678 GOSLING, S. N. and N. W. ARNELL. 2016. A global assessment of the impact of climate change on water
679   scarcity. *Climatic Change,* **134**(3), pp.371-385.

680 HAENSLER, A., F. SAEED and D. JACOB. 2013. Assessing the robustness of projected precipitation changes
681   over central Africa on the basis of a multitude of global and regional climate projections. *Climatic*
682   *Change,* **121**(2), pp.349-363.

683 HARRIS, I., P. JONES, T. OSBORN and D. LISTER. 2014. Updated high-resolution grids of monthly climatic
684   observations–the CRU TS3. 10 Dataset. *International Journal of Climatology,* **34**(3), pp.623-642.

685 KATZ, R. W., P. F. CRAIGMILE, P. GUTTORP, M. HARAN, B. SANSÓ and M. L. STEIN. 2013. Uncertainty analysis
686   in climate change assessments. *Nature Climate Change,* **3**(9), pp.769-771.

687 KNUTTI, R., R. FURRER, C. TEBALDI, J. CERMAK and G. A. MEEHL. 2010. Challenges in combining projections
688   from multiple climate models. *Journal of Climate,* **23**(10), pp.2739-2758.

689 KNUTTI, R. and J. SEDLÁČEK. 2013. Robustness and uncertainties in the new CMIP5 climate model
690   projections. *Nature Climate Change,* **3**(4), pp.369-373.

691 KOUTSOYIANNIS, D., A. EFSTRATIADIS and K. P. GEORGAKAKOS. 2007. Uncertainty Assessment of Future
692   Hydroclimatic Predictions: A Comparison of Probabilistic and Scenario-Based Approaches. *Journal*
693   *of Hydrometeorology,* **8**(3), pp.261-281.

694 LAUER, A. and K. HAMILTON. 2013. Simulating clouds with global climate models: A comparison of CMIP5
695   results with CMIP3 and satellite data. *Journal of Climate,* **26**(11), pp.3823-3845.

696 LE COZ, M., F. DELCLAUX, P. GENTHON and G. FAVREAU. 2009. Assessment of Digital Elevation Model (DEM)
697   aggregation methods for hydrological modeling: Lake Chad basin, Africa. *Computers & Geosciences,*
698   **35**(8), pp.1661-1670.

699 MANI, A. and F. T.-C. TSAI. 2016. Ensemble Averaging Methods for Quantifying Uncertainty Sources in
700   Modeling Climate Change Impact on Runoff Projection. *Journal of Hydrologic Engineering*,
701   p04016067.

MCSWEENEY, C., R. JONES, R. LEE and D. ROWELL. 2015. Selecting CMIP5 GCMs for downscaling over multiple regions. *Climate dynamics,* **44**(11-12), pp.3237-3260.

MEEHL, G. A., T. F. STOCKER, W. D. COLLINS, A. FRIEDLINGSTEIN, A. T. GAYE, J. M. GREGORY, A. KITOH, R. KNUTTI, J. M. MURPHY and A. NODA. 2007. Global climate projections.

MEHRAN, A., A. AGHAKOUCHAK and T. J. PHILLIPS. 2014. Evaluation of CMIP5 continental precipitation simulations relative to satellite-based gauge-adjusted observations. *Journal of Geophysical Research: Atmospheres,* **119**(4), pp.1695-1707.

MIAO, C., Q. DUAN, Q. SUN, Y. HUANG, D. KONG, T. YANG, A. YE, Z. DI and W. GONG. 2014. Assessment of CMIP5 climate models and projected temperature changes over Northern Eurasia. *Environmental Research Letters,* **9**(5), p055007.

MIN, S.-K. and A. HENSE. 2006. A Bayesian approach to climate model evaluation and multi-model averaging with an application to global mean surface temperatures from IPCC AR4 coupled climate models. *Geophysical Research Letters,* **33**(8), pp.n/a-n/a.

MONERIE, P. A., M. BIASUTTI and P. ROUCOU. 2016. On the projected increase of Sahel rainfall during the late rainy season. *International Journal of Climatology,* **36**(13), pp.4373-4383.

NGATCHA, B. N. 2009. Water resources protection in the Lake Chad Basin in the changing environment. *European Water,* **25**(26), pp.3-12.

NICHOLSON, S. E. 2009. A revised picture of the structure of the "monsoon" and land ITCZ over West Africa. *Climate dynamics,* **32**(7-8), pp.1155-1171.

NICHOLSON, S. E. 2013. The West African Sahel: A review of recent studies on the rainfall regime and its interannual variability. *ISRN Meteorology,* **2013**.

NICHOLSON, S. E. 2018. The ITCZ and the Seasonal Cycle over Equatorial Africa. *Bulletin of the American Meteorological Society,* **99**(2), pp.337-348.

NKIAKA, E., N. NAWAZ and J. C. LOVETT. 2017a. Evaluating Global Reanalysis Datasets as Input for Hydrological Modelling in the Sudano-Sahel Region. *Hydrology,* **4**(1), p13.

NKIAKA, E., N. R. NAWAZ and J. C. LOVETT. 2017b. Analysis of rainfall variability in the Logone catchment, Lake Chad basin. *International Journal of Climatology,* **37**(9), pp.3553-3564.

NKIAKA, E., N. R. NAWAZ and J. C. LOVETT. 2017c. Effect of single and multi-site calibration techniques on hydrological model performance, parameter estimation and predictive uncertainty: a case study in the Logone catchment, Lake Chad basin. *Stochastic environmental research and risk assessment,* 10.1007/s00477-017-1466-0.

OCHA. 2017. *Lake Chad Basin: Crisis Update*

ODADA, E., L. OYEBANDE and J. OGUNTOLA. 2009. *Lake Chad experience and lessons learned*.

OKPARA, U. T., L. C. STRINGER, A. J. DOUGILL and M. D. BILA. 2015. Conflicts about water in Lake Chad: Are environmental, vulnerability and security issues linked? *Progress in Development Studies,* **15**(4), pp.308-325.

PARK, J.-Y., J. BADER and D. MATEI. 2015. Northern-hemispheric differential warming is the key to understanding the discrepancies in the projected Sahel rainfall. *Nature communications,* **6**.

PATTNAYAK, K., S. KAR, M. DALAL and R. PATTNAYAK. 2017. Projections of annual rainfall and surface temperature from CMIP5 models over the BIMSTEC countries. *Global and Planetary Change,* **152**, pp.152-166.

PEEL, M. C., B. L. FINLAYSON and T. A. MCMAHON. 2007. Updated world map of the Köppen-Geiger climate classification. *Hydrol. Earth Syst. Sci.,* **11**(5), pp.1633-1644.

POLSON, D., M. BOLLASINA, G. HEGERL and L. WILCOX. 2014. Decreased monsoon precipitation in the Northern Hemisphere due to anthropogenic aerosols. *Geophysical Research Letters,* **41**(16), pp.6023-6029.

748 QUESADA, B., N. DEVARAJU, N. DE NOBLET-DUCOUDRÉ and A. ARNETH. 2017. Reduction of monsoon rainfall
749   in response to past and future land use and land cover changes. *Geophysical Research Letters,* **44**(2),
750   pp.1041-1050.
751 RAWLINS, M., R. S. BRADLEY and H. DIAZ. 2012. Assessment of regional climate model simulation estimates
752   over the northeast United States. *Journal of Geophysical Research: Atmospheres,* **117**(D23).
753 ROWELL, D. P. 2013. Simulating SST teleconnections to Africa: What is the state of the art? *Journal of*
754   *Climate,* **26**(15), pp.5397-5418.
755 SCHEWE, J., J. HEINKE, D. GERTEN, I. HADDELAND, N. W. ARNELL, D. B. CLARK, R. DANKERS, S. EISNER, B. M.
756   FEKETE and F. J. COLÓN-GONZÁLEZ. 2014. Multimodel assessment of water scarcity under climate
757   change. *Proceedings of the National Academy of Sciences,* **111**(9), pp.3245-3250.
758 SENGUPTA, A. and M. RAJEEVAN. 2013. Uncertainty quantification and reliability analysis of CMIP5
759   projections for the Indian summer monsoon. *Current Science*, pp.1692-1703.
760 SIAM, M. S., M.-E. DEMORY and E. A. B. ELTAHIR. 2013. Hydrological Cycles over the Congo and Upper Blue
761   Nile Basins: Evaluation of General Circulation Model Simulations and Reanalysis Products. *Journal*
762   *of Climate,* **26**(22), pp.8881-8894.
763 TANVEER, M. E., M.-H. LEE and D.-H. BAE. 2016. Uncertainty and Reliability Analysis of CMIP5 Climate
764   Projections in South Korea Using REA Method. *Procedia Engineering,* **154**, pp.650-655.
765 TAYLOR, C. M., D. BELUŠIĆ, F. GUICHARD, D. J. PARKER, T. VISCHEL, O. BOCK, P. P. HARRIS, S. JANICOT, C.
766   KLEIN and G. PANTHOU. 2017. Frequency of extreme Sahelian storms tripled since 1982 in satellite
767   observations. *Nature,* **544**(7651), pp.475-478.
768 TAYLOR, K. E., R. J. STOUFFER and G. A. MEEHL. 2012. An overview of CMIP5 and the experiment design.
769   *Bulletin of the American Meteorological Society,* **93**(4), pp.485-498.
770 TEBALDI, C. and R. KNUTTI. 2007. The use of the multi-model ensemble in probabilistic climate projections.
771   *Philosophical Transactions of the Royal Society of London A: Mathematical, Physical and Engineering*
772   *Sciences,* **365**(1857), pp.2053-2075.
773 TRENBERTH, K. E. 2011. Changes in precipitation with climate change. *Climate Research,* **47**(1-2), pp.123-
774   138.
775 WASHINGTON, R., M. C. TODD, S. ENGELSTAEDTER, S. MBAINAYEL and F. MITCHELL. 2006. Dust and the low-
776   level circulation over the Bodélé Depression, Chad: Observations from BoDEx 2005. *Journal of*
777   *Geophysical Research: Atmospheres,* **111**(D3).
778 WEEDON, G. P., G. BALSAMO, N. BELLOUIN, S. GOMES, M. J. BEST and P. VITERBO. 2014. The WFDEI
779   meteorological forcing data set: WATCH Forcing Data methodology applied to ERA-Interim
780   reanalysis data. *Water Resources Research,* **50**(9), pp.7505-7514.
781 WEHNER, M. 2013. Methods of Projecting Future Changes in Extremes. *In:* A. AGHAKOUCHAK, D.
782   EASTERLING, K. HSU, S. SCHUBERT and S. SOROOSHIAN, eds. *Extremes in a Changing Climate:*
783   *Detection, Analysis and Uncertainty.* Dordrecht: Springer Netherlands, pp.223-237.
784 WOLDEMESKEL, F., A. SHARMA, B. SIVAKUMAR and R. MEHROTRA. 2012. An error estimation method for
785   precipitation and temperature projections for future climates. *Journal of Geophysical Research:*
786   *Atmospheres,* **117**(D22).

787

788